VARIATION IN THE ^{64}Ge$(p,\gamma)^{65}$As REACTION RATES

N.T.T. Quyen

Faculty of Fundamental Sciences, Van Lang University
Ho Chi Minh City 700000, Vietnam

N.N. Duy[†]

Department of Physics, Sungkyunkwan University, Suwon 16419, South Korea

N.K. Uyen

Department of Physics, Sungkyunkwan University, Suwon 16419, South Korea

T.V. Nhan Hao

Faculty of Physics, University of Education, Hue University
34 Le Loi Street, Hue City 530000, Vietnam

(Received October 30, 2020; accepted March 25, 2021)

We report on the variation in the ^{64}Ge$(p,\gamma)^{65}$As reaction rates due to uncertainties of either nuclear mass and level structure of the ^{65}As isotope or non-resonant reaction rates. The change in the reaction rates is from a few factors to one order of magnitude due to the uncertainty of the non-resonant rates, which were calculated using the astrophysical S-factor and the statistical Hauser–Feshbach model. The mass uncertainty of the ^{65}As nucleus ($\Delta m = 85$ keV) results in a variation of a few factors in the reaction rates at $T_9 = 1$. At present, the estimated effective lifetimes of ^{64}Ge in the rp-process are ranging from 0.5 to 162 ms. The results indicate that the resonance at $E_x = 1.155$ MeV and the Q-value of the reaction must be precisely determined to improve the accuracy of rp-process simulations.

DOI:10.5506/APhysPolB.52.291

1. Introduction

The thermonuclear explosion in X-ray bursts (XRBs) [1–4] is triggered by the hot hydrogen burning in which the seed nuclei rapidly capture protons to synthesize heavier isotopes, namely the rp-process [4]. This process is

[†] Corresponding author: ngocduydl@gmail.com; ngocduydl@skku.edu

believed to occur on accretion disks of neutron stars or black holes [5]. During the explosions, the reaction flows shift towards the proton dripline via the proton captures. However, the process of proton addition has to overcome the increased Coulomb barriers once it produces heavier isotopes. Subsequently, there is a competition between β^+-decay, proton capture (p,γ), and photodisintegration (γ,p) in the rp-process. If the reaction flow cannot proceed further, the nucleosynthesis awaits the β^+-decay at a long-lived nucleus, so-called waiting point, and a (p,γ)–(γ,p) equilibrium can be established. Since the waiting points have half-lives [6] compatible with the XRB duration (10–100 s), the proton captures and photodisintegrations of these isotopes and their neighbors are sensitive to the XRB calculations, such as luminosity of the light curves or isotopic abundance [7–10].

The rp-process is thought to be extinguished around the Sn–Sb–Te cycles [11, 12]. The evolution proceeds through the ^{64}Ge (63.7 s), ^{68}Se (35.5 s), and ^{72}Kr (17.2 s) [6] waiting points. The slow decay of these waiting points temporarily impacts the XRB light curves with rapid proton captures during their effective lifetimes. Once the (p,γ)–(γ,p) equilibrium is established, these long lifetime waiting points can produce bottlenecks in the rp-process, which slows down the proton captures. The waiting points can also be bypassed by two-proton captures, which reduce the effective lifetime of these nuclei [13]. Subsequently, the proton captures (and their reverse reactions) play an important role in understanding the reaction paths proceeding through these waiting points. For instance, the study by Parikh *et al.* [14] reported that astrophysical rate variations in the ^{64}Ge$(p,\gamma)^{65}$As reactions strongly affect the abundance of the isotopes in the range of $A = 64$–80, which were calculated by ten XRB models. Besides, a series of studies by Cyburt *et al.* [7] and Parikh *et al.* [8, 9, 14] stated that the proton capture of the ^{64}Ge isotope strongly impacts the XRB calculations.

Although the ^{64}Ge$(p,\gamma)^{65}$As reaction rates are important to evaluate the evolution of the rp-process, its astrophysical rates are still uncertain. The recent work by Lam *et al.* [15] investigated the reaction rates using five resonances calculated using shell model and direct-capture rate based on astrophysical S-factor. The mass uncertainty of 85 keV of ^{65}As was taken into account for the resonant rate calculations. However, comparing to the level structure of the mirror nucleus (^{65}Ge) [16], under stellar condition of $T_9 = 0$–2, which corresponds to the energy range of $E_x = 0$–1.5 MeV, more resonances are expected to exist in the ^{65}As nucleus. Besides, the non-resonant rates of this reaction can also be determined using the statistical Hauser–Feshbach model [17] if a continuing spectrum exists just above the proton emission threshold ($Q = -0.09$ MeV) in ^{65}As. Therefore, in this study, we investigate the resonant rates by taking two resonances of $E_x = 1.155$ and 1.215 MeV from the mirror nucleus [18] together with the

five resonances taken from the shell model calculations in Ref. [15]. The non-resonant rates estimated using the statistical Hauser–Feshbach model are compared to those based on the direct-capture method obtained from Ref. [15]. Subsequently, the variation in the ^{64}Ge$(p,\gamma)^{65}$As reaction rates and the effective lifetime and strength of the waiting point at ^{64}Ge are evaluated with new reaction rates.

2. Theoretical framework

Proton-capture rates of an isotope in the rp-process are considered as a sum of resonant (r) and non-resonant (nr) rates. The numerical calculation for resonant rates ($N_A\langle\sigma\nu\rangle_{\rm r}$) of the ^{64}Ge$(p,\gamma)^{65}$As reaction is given by [19]

$$N_A\langle\sigma\nu\rangle_{\rm r} = 11.54\times10^{11}(\mu T_9)^{-3/2}\sum\omega\gamma_i\times\exp\left(\frac{-11.605E_i}{T_9}\right)\left[\mathrm{cm^3s^{-1}mol^{-1}}\right], \tag{1}$$

where μ (in amu), T_9 (in GigaKelvin — GK), and $\omega\gamma_i$ are the reduced mass of the entrance channel, the temperature of the stellar environment, and the resonant strength of resonance E_i (in MeV) of the compound nucleus, respectively. The energy of resonance is simply determined as $E_i = E_x - Q$ with E_x and Q being excitation energy and Q-value of the reaction. Obviously, the resonant rates are very sensitive to the Q-value (or nuclear mass) of the reaction.

While the resonant rates are calculated using resonances of the compound nucleus that the reaction proceeds through, the non-resonant rates can be estimated using the statistical Hauser–Feshbach model or the astrophysical S-factor at the Gamow energy E_0. For the latter (direct-capture) method, the non-resonant rates are calculated by [20]

$$N_A\langle\sigma\nu\rangle_{\rm nr} = 7.83\times10^{9}\left(\frac{Z_{\rm t}}{\mu T_9^2}\right)^{1/3}S(E_0)\exp\left[-4.249\left(\frac{Z_{\rm t}^2\mu}{T_9}\right)^{1/3}\right]\left[\mathrm{cm^3s^{-1}mol^{-1}}\right], \tag{2}$$

where $Z_{\rm t}$ is the atomic number of the target (^{64}Ge). The astrophysical S-factor reads

$$S(E_0) = S(0)\left[1+\frac{5}{12}\frac{\left(Z_t^2\mu/T_9\right)^{1/3}}{4.2487}\right]\ [\mathrm{MeV\,b}], \tag{3}$$

where $S(0)$ is the astrophysical S-factor at zero energy, which is calculated using RADCAP [21]. If the level density above the proton-emission threshold ($S_p = -0.09$ MeV) in the compound nucleus (^{65}As) is high (*i.e.*, 5–10 levels/MeV), the non-resonant rates can be estimated using the

statistical Hauser–Feshbach model [17]. Hence, we also employed the NON-SMOKER code [17] to compute the (statistical) non-resonant rates. Finally, the total proton-capture rates can be determined by $N_A\langle\sigma\nu\rangle = N_A\langle\sigma\nu\rangle_{\rm r} + N_A\langle\sigma\nu\rangle_{\rm nr}$.

Taking the reaction rates, the proton-capture effective lifetime of ^{64}Ge in the rp-process can be estimated by [20]

$$\frac{1}{\tau_{p\gamma}} = \frac{1}{\tau_{\rm r}} + \frac{1}{\tau_{\rm nr}} = \rho\chi_p N_A\langle\sigma\nu\rangle_{\rm r} + \rho\chi_p N_A\langle\sigma\nu\rangle_{\rm nr}\ \left[{\rm s}^{-1}\right], \tag{4}$$

where $\tau_{p\gamma}$, $\tau_{\rm r}$, and $\tau_{\rm nr}$ are the proton-capture lifetime of reaction target, the lifetimes associated with the resonant, and non-resonant rates, respectively; ρ and χ_p are the stellar matter density (in g/cm^3) and the hydrogen fraction in such stellar matter, respectively. Obviously, variations in non-resonant and/or resonant rates will impact the effective lifetime.

The variation in the resonant rates is mainly due to the uncertainty of the Q-value of the (p,γ) reaction. An uncertainty ΔQ of the Q-value will result in a change of $\Delta E_i = \Delta Q$, leading to a large variation in the resonant rates. Taking Eqs. (1) and (4), the variation in the resonant-capture effective lifetime is given by

$$\tau_{\rm r}^{*} = \exp\left(\frac{\pm 11.605\Delta Q}{T_9}\right)\tau_{\rm r}\,, \tag{5}$$

where $\tau_{\rm r}^{*} = 1/[\rho\chi_p N_A^{*}\langle\sigma\nu\rangle_{\rm r}]$ with $N_A^{*}\langle\sigma\nu\rangle_{\rm r}$ being the resonant rates associated with $Q^{*} = Q + \Delta Q$ or $Q^{*} = Q - \Delta Q$.

In this work, the Q-value of the ^{64}Ge$(p,\gamma)^{65}$As reaction and its uncertainty are calculated using the recent updated mass database, AME2016 [22]. Subsequently, the variations in the reaction rates and effective lifetime of ^{64}Ge, due to uncertainties of Q-value (or mass) or non-resonant rates, are determined. Furthermore, the competition between the proton capture and the β^{+}-decay at ^{64}Ge is evaluated using $\tau_{p\gamma}$ and β^{+}-decay lifetime $\tau_{\beta^{+}} = T_{1/2}/\ln 2$ with $T_{1/2} = 63.7$ s [6] to determine the strength of the rp-process waiting point at this isotope.

3. Results and discussion

The resonant rates of the ^{64}Ge$(p,\gamma)^{65}$As reaction were calculated using the resonances in ^{65}As predicted using the shell model calculations [15] and the information of the mirror nucleus (^{65}Ge) [18]. Table I is a summary of seven resonant states of interest, which ranges from $E_i = 0$ to 1.2 MeV corresponding to the Gamow windows at stellar temperatures of $T_9 = 0.01$–2. Using the formalism in Eq. (1), we determined the astrophysical rates of each resonance, which are listed in Table II.

TABLE I

Summary of resonances in the ^{64}Ge$(p,\gamma)^{65}$As reaction, which were taken from Refs. [15, 18]. The resonant energy, E_i, was calculated using the recent proton separation energy $Q = -0.09$ MeV adopted from AME2016 database [22]. [(a)] and [(b)] denote excitation energies that were measured by Obertelli *et al.* [23] and taken from Ref. [18], respectively.

ID	E_x [MeV]	E_i [MeV]	J^π	$\omega\gamma$ [eV]
1	0.187	0.277	$5/2^-$	2.46×10^{-16} [(a)]
2	0.501	0.591	$5/2^-$	1.13×10^{-9}
3	0.863	0.953	$5/2^-$	4.89×10^{-6}
4	0.947	1.037	$7/2^-$	4.88×10^{-5}
5	1.070	1.160	$7/2^-$	3.27×10^{-5}
6	1.155	1.245	$7/2^-$	1.30×10^{-3} [(b)]
7	1.215	1.305	$9/2^-$	1.90×10^{-6} [(b)]

TABLE II

Resonant rates (in cm^{3}s^{-1}mol^{-1}) calculated using seven resonances from Table I at different stellar temperatures.

T_9 (GK)	$E_i = 0.277$	0.591	0.953	1.037	1.160	1.245	1.305 [MeV]
0.1	1.34E-23	9.21E-33	2.27E-47	1.32E-50	5.60E-57	1.16E-59	1.60E-65
0.2	4.54E-17	2.55E-18	8.31E-24	6.34E-25	3.38E-28	9.68E-29	4.35E-33
0.3	5.24E-15	1.28E-13	4.58E-16	1.77E-16	1.02E-18	1.51E-18	2.17E-22
0.4	4.96E-14	2.52E-11	2.99E-12	2.61E-12	4.93E-14	1.67E-13	4.27E-17
0.5	1.77E-13	5.56E-10	5.40E-10	7.67E-10	2.96E-11	1.64E-10	5.94E-14
0.6	3.93E-13	4.16E-09	1.64E-08	3.22E-08	2.00E-09	1.54E-08	7.03E-12
0.7	6.71E-13	1.69E-08	1.81E-07	4.49E-07	3.91E-08	3.80E-07	2.05E-10
0.8	9.75E-13	4.71E-08	1.07E-06	3.15E-06	3.54E-07	4.11E-06	2.51E-09
0.9	1.28E-12	1.02E-07	4.16E-06	1.40E-05	1.93E-06	2.56E-05	1.73E-08
1	1.56E-12	1.87E-07	1.21E-05	4.57E-05	7.34E-06	1.09E-04	7.93E-08
1.5	2.48E-12	1.00E-06	2.63E-04	1.37E-03	3.55E-04	7.32E-03	6.72E-06
2	2.75E-12	2.04E-06	1.08E-03	6.63E-03	2.17E-03	5.28E-02	5.45E-05

To evaluate the key resonances that the ^{64}Ge$(p,\gamma)^{65}$As reaction proceeds through, the contributions of each state i to the total resonant rates $(N_A\langle\sigma\nu\rangle_{\rm r}^{\rm 7res})$ were estimated by the ratio of $N_A^i\langle\sigma\nu\rangle_{\rm r}/N_A\langle\sigma\nu\rangle_{\rm r}^{\rm 7res}$. The visual results of the contributions are shown in Fig. 1 (a). In the range of $T_9 > 0.3$, the contributions of the resonances at $E_x = 0.187$ and 1.070 MeV can be negligible, whereas the state at $E_x = 0.187$ MeV significantly contributes to the rates. The 1.215-MeV state mostly does not impact the rates in the whole range of stellar temperature. However, the reaction strongly proceeds through the sixth level, $E_x = 1.155$ MeV, when temperatures exceed 0.5 GK. When $T_9 < 0.5$, the second resonance takes an important part

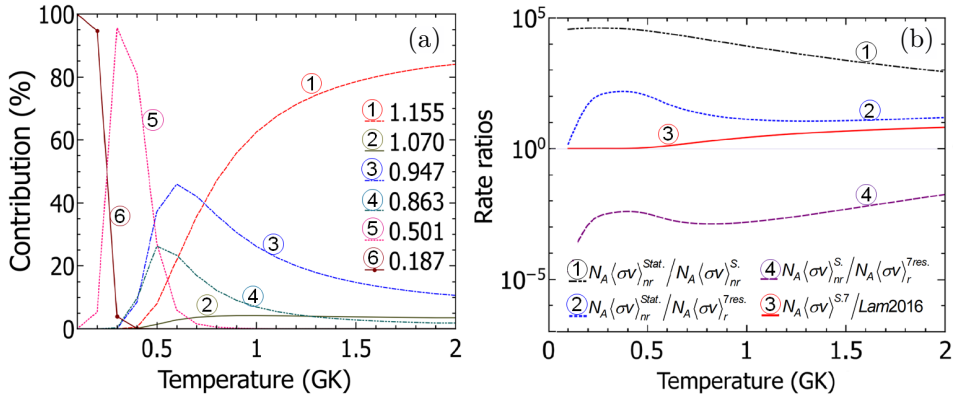

Fig. 1. (Color online) (a) Contributions of resonances to the total resonant rate of the ^{64}Ge$(p,\gamma)^{65}$As reaction in the temperature range of $T_9 = 0.1$–2. The contribution of the level at $E_x = 1.215$ MeV (black curve (2)) cannot be seen because it is approximately equal to zero. (b) Ratios for comparisons of proton-capture rates (non-resonant and resonant). Notice that $N_A\langle\sigma\nu\rangle^{\rm stat}_{\rm nr}$: non-resonant rates of statistical Hauser–Feshbach model (NON-SMOKER code); $N_A\langle\sigma\nu\rangle^{\rm S}_{\rm nr}$: non-resonant rates based on S-factor; $N_A\langle\sigma\nu\rangle^{7\rm res}_{\rm r}$: total resonant rates; $N_A\langle\sigma\nu\rangle^{\rm S\,7}$ (thick red curve (3)): $N_A\langle\sigma\nu\rangle^{\rm S}_{\rm nr} + N_A\langle\sigma\nu\rangle^{7\rm res}_{\rm r}$ rates; and *Lam*2016: total rates calculated in Ref. [15].

in the rate contribution. The first state only significantly contributes to the rates under the condition of $T_9 < 0.3$. In the range of $T_9 = 0.4$–1.5, the main contributions are observed for the resonances at $E_x = 0.863$ and 0.947 MeV. In general, the results indicate that the ^{64}Ge$(p,\gamma)^{65}$As reaction mainly proceeds through only five resonances at $E_x = 0.187$, 0.501, 0.863, 0.947, and 1.155 MeV under typical XRB temperature of $T_9 = 0.5$–1. It should be noted that although high-energy resonances, in principle, are less important than low-energy ones as shown in the relationship of Eq. (1), the 1.155-MeV level has a strong contribution to the rates compared to lower levels (*i.e.*, $E_x = 0.863, 0.947$ MeV). This result can be explained by the power of its resonant strength ($\omega\gamma$), which is about 2 orders of magnitude stronger than those of the other resonances. Hence, both the resonant strength and resonant energy must be precisely determined at the same time for improving the accuracy of the resonant rate estimations.

Table III presents the total resonant rates, including their variations due to the mass uncertainty and non-resonant rates, which were computed using the statistical Hauser–Feshbach model and the direct-capture method. For the non-resonant rates calculated using the latter approach, the S-factor at zero energy of about $S(0) = 35$ MeV b, which is similar to that obtained in Ref. [15], was reproduced using the RADCAP code [21]. Hence, the direct-capture non-resonant rates in the present study are equivalent to those in the

TABLE III

Total resonant rates contributed by seven resonances and non-resonant rates calculated using the statistical Hauser–Feshbach model and the direct-capture method. Notice that all the rates are in the unit of $cm^3s^{-1}mol^{-1}$. Lower and Upper denote the variations in the total resonant rates due to Q-value changes of $Q^* = Q+85$ keV and $Q^* = Q - 85$ keV, respectively.

T_9 [GK]	Lower	$N_A\langle\sigma\nu\rangle_{\rm r}^{\rm 7res}$	Upper	$N_A\langle\sigma\nu\rangle_{\rm nr}^{\rm S}$	$N_A\langle\sigma\nu\rangle_{\rm nr}^{\rm stat}$
0.1	6.98E-28	1.34E-23	2.58E-19	5.54E-28	2.02E-23
0.2	3.45E-19	4.79E-17	6.64E-15	5.85E-20	2.38E-15
0.3	4.99E-15	1.34E-13	3.58E-12	4.46E-16	1.81E-11
0.4	2.64E-12	3.10E-11	3.66E-10	1.24E-13	4.67E-09
0.5	2.86E-10	2.06E-09	1.48E-08	6.75E-12	2.16E-07
0.6	1.35E-08	7.01E-08	3.63E-07	1.42E-10	3.60E-06
0.7	2.61E-07	1.07E-06	4.36E-06	1.60E-09	3.13E-05
0.8	2.54E-06	8.73E-06	3.00E-05	1.19E-08	1.75E-04
0.9	1.53E-05	4.58E-05	1.37E-04	6.41E-08	7.13E-04
1	6.50E-05	1.74E-04	4.67E-04	2.74E-07	2.31E-03
1.5	4.83E-03	9.31E-03	1.80E-02	4.57E-05	1.09E-01
2	3.83E-02	6.27E-02	1.03E-01	1.13E-03	9.80E-01

previous work [15]. In Fig. 1 (b), we show comparisons of the non-resonant rates calculated using the statistical Hauser–Feshbach model ($N_A\langle\sigma\nu\rangle_{\rm nr}^{\rm stat}$) to those computed using the direct-capture method ($N_A\langle\sigma\nu\rangle_{\rm nr}^{\rm S}$) and the non-resonant rates to the total resonant rates ($N_A\langle\sigma\nu\rangle_{\rm r}^{\rm 7res}$). Notice that there are two sets of total reaction rates, which were determined by $N_A\langle\sigma\nu\rangle^{\rm stat7} = N_A\langle\sigma\nu\rangle_{\rm nr}^{\rm stat} + N_A\langle\sigma\nu\rangle_{\rm r}^{\rm 7res}$ and $N_A\langle\sigma\nu\rangle^{\rm S\,7} = N_A\langle\sigma\nu\rangle_{\rm nr}^{\rm S} + N_A\langle\sigma\nu\rangle_{\rm r}^{\rm 7res}$. The total rates of $N_A\langle\sigma\nu\rangle^{\rm S\,7}$ were also compared to those estimated in Ref. [15]. The results indicate that there is a large, more than 3 orders of magnitude, discrepancy between $N_A\langle\sigma\nu\rangle_{\rm nr}^{\rm stat}$ and $N_A\langle\sigma\nu\rangle_{\rm nr}^{\rm S}$. In addition, the statistical Hauser–Feshbach model overestimates the resonant rates by a factor of 10–100, while the direct-capture method underestimates the resonant rates by 2–3 orders of magnitude. Therefore, the total rates are approximately equal to the statistical (or resonant) rates if the non-resonant rates are considered by the statistical Hauser–Feshbach model (or the direct-capture method). In other words, we have $N_A\langle\sigma\nu\rangle^{\rm stat7} \approx N_A\langle\sigma\nu\rangle_{\rm nr}^{\rm stat}$ and $N_A\langle\sigma\nu\rangle^{\rm S\,7} \approx N_A\langle\sigma\nu\rangle_{\rm r}^{\rm 7res}$. Moreover, the total rates ($N_A\langle\sigma\nu\rangle^{\rm S\,7}$) calculated in the present study are from a few factors to one order of magnitude higher than those obtained in Ref. [15]. This discrepancy is mainly due to the contribution of the resonance at $E_x = 1.155$ MeV, which was ignored in the previous study by Lam *et al.* [15]. As a consequence, this level must be confirmed for better predictions of the resonant rates of the ^{64}Ge$(p,\gamma)^{65}$As reaction.

Obviously, the total rates of the ^{64}Ge$(p,\gamma)^{65}$As reaction are very uncertain owing to the uncertainties in the estimations of non-resonant rates and ambiguity of the 1.155-MeV state. Therefore, measurements for nuclear structure above the proton-emission threshold ($Q = -0.09$ MeV) of the ^{65}As nucleus are highly demanded. Since the statistical Hauser–Feshbach model and the direct-capture method strongly depend on the level density and the interaction potential of a colliding system, respectively, the level scheme of ^{65}As and interaction parameters (*i.e.*, nuclear central potential, depth of spin-orbit potential, interacting radius, *etc.*, which are in models for cross-section calculations [21, 24]) of the ^{64}Ge+p system must be precisely determined. For instance, the mentioned parameters in the optical potential model [24] can be deduced by fitting theoretical calculations to measured cross sections of reactions. At present, it is difficult to conclude if the statistical Hauser–Feshbach model or the direct-capture method can be well applied to the calculations due to the lack of level scheme of the ^{65}As nucleus. If ^{65}As has high-level density in the energy range of interest ($E_x = 0$–1.2 MeV), the statistical Hauser–Feshbach model is reliable for estimating the non-resonant rates, otherwise, the direct-capture method should be utilized.

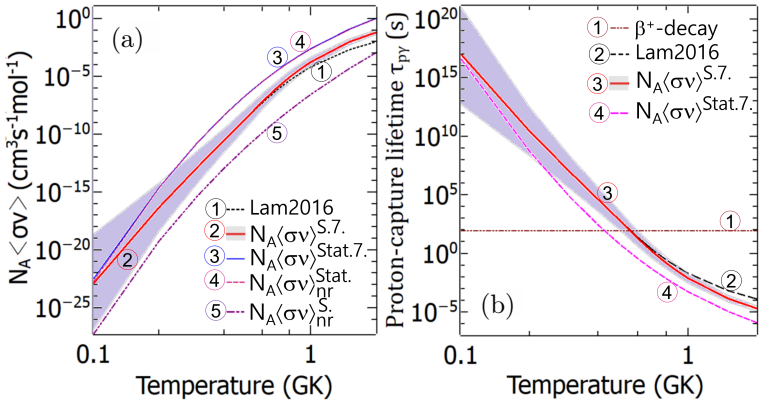

Fig. 2. (Color online) (a) Reaction rates calculated using different methods. Notice that $N_A\langle\sigma\nu\rangle^{\rm stat7} = N_A\langle\sigma\nu\rangle^{\rm stat}_{\rm nr} + N_A\langle\sigma\nu\rangle^{\rm 7res}_{\rm r}$ (thin blue curve (3)) $\approx N_A\langle\sigma\nu\rangle^{\rm stat}_{\rm nr}$ (pink dashed curve (4)) because $N_A\langle\sigma\nu\rangle^{\rm stat}_{\rm nr} \gg N_A\langle\sigma\nu\rangle^{\rm 7res}_{\rm r}$. (b) Effective lifetimes (in seconds) of ^{64}Ge in the rp-process were calculated using reaction rates shown in the right panel of Fig. 1 (b) under the typical XRB condition of $\rho = 10^6$ g/cm^3 and $\chi_p = 0.75$. The shaded areas indicate the rate and lifetime variations due to mass uncertainty of the ^{65}As isotope.

We found that the variations in the ^{64}Ge$(p,\gamma)^{65}$As reaction rates are caused by the uncertainties not only in the non-resonant rate calculations and the missing resonances but also in the nuclear mass of ^{65}As. With the

^{65}As mass uncertainty of $\Delta m = 85$ keV, the resonant rates change by a few and 1–2 orders of magnitude at temperatures in the range of $T_9 < 0.5$ and $T_9 = 0.5$–2, respectively, as indicated by the shaded area in Fig. 2 (a). By considering the reaction rates associated with $Q^* = Q - 85$ keV (upper rates of the shaded area), the resonant rates ($N_A\langle\sigma\nu\rangle_{\rm r}^{\rm 7res}$) underestimate the statistical ones ($N_A\langle\sigma\nu\rangle_{\rm nr}^{\rm stat}$) with $T_9 > 0.25$, and *vice versa* with $T_9 < 0.25$. For the Q-value of $Q^* = Q + 85$ keV (lower rates of the shaded area), the resonant rates are almost similar to the non-resonant rates calculated using S-factor.

To evaluate the impact of the reaction rate variation on the existing time of ^{64}Ge in the rp-process, the proton-capture lifetime (in seconds) of this isotope was calculated under the typical XRB conditions of $\rho = 10^6$g/cm^3 and $\chi_p = 0.75$. As shown in Fig. 2 (b), the variation in the reaction rates leads to a significant change in the effective lifetime of the ^{64}Ge nucleus. Subsequently, it is difficult to determine the dominant between the proton capture and β^+-decay at ^{64}Ge. The upper and lower rates of the shaded area correspond to the lower and upper lifetimes estimated with the mass uncertainties of $Q^* = Q - 85$ keV and $Q^* = Q + 85$ keV, respectively. We found that the balance between the proton capture and the decay is established at $T_9 = 0.6$ for $Q^* = Q + 85$ keV, but at $T_9 = 0.45$ for $Q^* = Q - 85$ keV. As a consequence, the balance point shifts by 150 MK, leading to uncertainty in determination of the branching at ^{64}Ge in the reaction flow. In addition, the variations in the non-resonant rates also result in an uncertainty of 200 MK in determination of the temperature point at which the balance is established.

Taking the total reaction rates based on seven resonances and S-factor ($N_A\langle\sigma\nu\rangle^{\rm S\,7}$) together with the ^{65}As mass uncertainty of 85 keV, the proton-capture effective lifetime of ^{64}Ge at $T_9 = 1$ is about $\tau_{p\gamma} = 3$–20 ms, whereas it is 62–182 ms and 0.5 ms if the reaction rates obtained from Ref. [15] and total rates $N_A\langle\sigma\nu\rangle^{\rm stat7}$ are, respectively, taken into account. The proton-capture lifetime of ^{64}Ge is also about 4 orders of magnitude shorter than the β-decay lifetime when $T_9 = 1$. In such a scenario, if the proton capture of ^{64}Ge can compete with its reverse reaction, ^{65}As$(\gamma,p)^{64}$Ge, the reaction flow can proceed through ^{64}Ge via the ^{64}Ge$(p,\gamma)^{65}$As$(p,\gamma)^{66}$Se reaction, leading to a weak waiting point of ^{64}Ge when $T_9 \geq 1$. In addition, the lifetime based on $N_A\langle\sigma\nu\rangle^{\rm S\,7}$ at $T_9 = 1$ in the present study is about 3 orders of magnitude shorter than those determined using $2p$-proton-capture rates of ^{64}Ge [25] and using calculations of proton separation energy of ^{65}As [26]. Since the XRB light curves strongly depend on the effective lifetimes of waiting points, reductions of ^{64}Ge lifetime uncertainty are also desirable.

The analyses above indicate that the variations in the ^{64}Ge$(p,\gamma)^{65}$As rates due to uncertainties of ^{65}As mass and non-resonant rates strongly impact determinations of the effective lifetime and the strength of the ^{64}Ge waiting point in the rp-process. Therefore, precise masses and level structure of ^{65}As are very important to narrow the uncertainties in XRB simulations. Notice that with the β^+-decay half-life of about 170 ms [6], measurements for ^{65}As are mostly possible at present accelerator facilities. For instance, with an accuracy level of 0.1 part-per-million and a measuring timescale of about 10 milliseconds, the Multiple-Reflection Time-of-Flight (MR-TOF) technique [27, 28] is reasonable to be employed for such measurements. Recently, MR-TOF systems have become available in modern accelerator facilities, such as BigRIPS [27], RAON [29], and TITAN [30]. We strongly suggest a precise mass measurement for the ^{65}As isotope. Moreover, studies of the nuclear structure above the proton threshold of ^{65}As can be feasible due to developments of radioactive ion beams at the recent facilities.

4. Conclusion

In this work, we investigated the variations in the resonant and non-resonant rates of the ^{64}Ge$(p,\gamma)^{65}$As reaction in the rp-process. The resonant rates in the present study are about one order of magnitude higher than those estimated in the previous work [15] due to the strong contribution of the resonance at $E_x = 1.155$ MeV. The non-resonant rates calculated using the statistical Hauser–Feshbach model are about 3–4 orders of magnitude higher than those estimated using the direct-capture method with the astrophysical S-factor. As a consequence, the astrophysical rates of the studied reaction vary by 1–2 orders of magnitude, leading to a large uncertainty in the effective lifetime of ^{64}Ge, which is from a few to tens of milliseconds. The $p\gamma$ lifetime determined in the present study indicates that ^{64}Ge is not a significant waiting point in the rp-process under typical XRB conditions. In addition, the establishment of the (p,γ)–β^+-decay balance at ^{64}Ge also shifts by 150–200 MK. The results show that measurements for both the precise mass and level structure of ^{65}As are highly desirable to reduce the variation in the ^{64}Ge$(p,\gamma)^{65}$As reaction rates. Finally, this study provides useful information for further studies on the properties of X-ray bursts and nucleosynthesis in stars.

This work was supported by the National Research Foundation of Korea (NRF) grant funded by the Korean Ministry of Education, Science, and Technology (MEST, No. NRF-2020R1C1C1006029). T.V. Nhan Hao (tvnhao@hueuni.edu.vn) also acknowledges the support of the Hue University under the Core Research Program, grant No. NCM.DHH.2018.09.

REFERENCES

[1] H. Herndl *et al.*, «Proton capture reaction rates in the rp process», *Phys. Rev. C* **52**, 1078 (1995).

[2] R.E. Taam, «Nuclear Processes at Neutron Star Surfaces», *Annu. Rev. Nucl. Sci.* **35**, 1 (1985).

[3] R.E. Taam *et al.*, «Successive X-Ray Bursts from Accreting Neutron Stars», *Astrophys. J.* **413**, 324 (1993).

[4] R.K. Wallace, S.E. Woosley, «Explosive hydrogen burning», *Astrophys. J. Suppl. Ser.* **45**, 389 (1981).

[5] W.H.G. Lewin *et al.*, «X-ray bursts», *Space Sci. Rev.* **62**, 223 (1993).

[6] G. Audi *et al.*, «The Nubase2012 evaluation of nuclear properties», *Chin. Phys. C* **36**, 1157 (2012).

[7] R.H. Cyburt *et al.*, «Dependence of X-Ray Burst Models on Nuclear Reaction Rates», *Astrophys. J.* **830**, 55 (2016).

[8] A. Parikh *et al.*, «The Effects of Variations in Nuclear Processes on Type I X-Ray Burst Nucleosynthesis», *Astrophys. J. Suppl. Ser.* **178**, 110 (2008).

[9] A. Parikh *et al.*, «Classical novae and type I X-ray bursts: Challenges for the 21st century», *AIP Advances* **4**, 041002 (2014).

[10] Z. Meisel *et al.*, «Influence of Nuclear Reaction Rate Uncertainties on Neutron Star Properties Extracted from X-Ray Burst Model — Observation Comparisons», *Astrophys. J.* **872**, 84 (2019).

[11] H. Schatz *et al.*, «End Point of the rp Process on Accreting Neutron Stars», *Phys. Rev. Lett.* **86**, 3471 (2001).

[12] V.-V. Elomaa *et al.*, «Quenching of the SnSbTe Cycle in the rp Process», *Phys. Rev. Lett.* **102**, 252501 (2009).

[13] H. Schatz *et al.*, «rp-process nucleosynthesis at extreme temperature and density conditions», *Phys. Rep.* **294**, 167 (1998).

[14] A. Parikh *et al.*, «Impact of uncertainties in reaction Q values on nucleosynthesis in type I X-ray bursts», *Phys. Rev. C* **79**, 045802 (2009).

[15] Y.H. Lam *et al.*, «Reaction Rates of ^{64}Ge$(p,\gamma)^{65}$As and As$(p,\gamma)^{66}$Se and the Extent of Nucleosynthesis in Type I X-Ray Bursts», *Astrophys. J.* **818**, 78 (2016).

[16] E. Browne, J.K. Tuli, «Nuclear Data Sheets for $A = 65$», *Nucl. Data Sheets* **111**, 2425 (2010).

[17] T. Rauscher, F.-K. Thielemann, «Astrophysical Reaction Rates From Statistical Model Calculations», *Atom. Data Nucl. Data Tables* **75**, 1 (2000).

[18] L. Van Wormer *et al.*, «Reaction Rates and Reaction Sequences in the rp-Process», *Astrophys. J.* **432**, 326 (1994).

[19] C. Iliadis, «Nuclear Physics of Stars», *Wiley*, 2007.

[20] C.E. Rolfs, W.S. Rodney, «Cauldrons in the Cosmos», *Nuclear Astrophysics University of Chicago Press*, 1988.

[21] C.A. Bertulani, «RADCAP: A potential model tool for direct capture reactions», *Comput. Phys. Commun.* **156**, 123 (2003).

[22] M. Wang *et al.*, «The AME2016 atomic mass evaluation (II). Tables, graphs and references», *Chin. Phys. C* **41**, 030003 (2017).

[23] A. Obertelli *et al.*, «First spectroscopy of ^{66}Se and ^{65}As: Investigating shape coexistence beyond the $N = Z$ line», *Phys. Lett. B* **701**, 417 (2011).

[24] J.T. Huang *et al.*, «Radiative capture of nucleons at astrophysical energies with single-particle states», *Atom. Data Nucl. Data Tables* **96**, 824 (2010).

[25] H. Schartz, «The importance of nuclear masses in the astrophysical rp-process», *Int. J. Mass Spectr.* **251**, 293 (2006).

[26] B.A. Brown *et al.*, «Proton dripline calculations and the rp process», *Phys. Rev. C* **65**, 045802 (2002).

[27] Y. Ishida *et al.*, «A multi-reflection time-of-flight mass spectrometer for mass measurements of short-lived nuclei», *Nucl. Instrum. Methods Phys. Res. B* **241**, 983 (2005).

[28] S. Schury *et al.*, «A high-resolution multi-reflection time-of-flight mass spectrograph for precision mass measurements at RIKEN/SLOWRI», *Nucl. Instrum. Methods Phys. Res. B* **335**, 39 (2014).

[29] Y.J. Kim, «Current status of experimental facilities at RAON», *Nucl. Instrum. Methods Phys. Res. B* **463**, 408 (2020).

[30] T. Dickel *et al.*, «Recent upgrades of the multiple-reflection time-of-flight mass spectrometer at TITAN, TRIUMF», *Hyperfine Interact.* **240**, 62 (2019).